

The Gas-Phase Reaction Between Hydroxide Ion and Methyl Formate: A Theoretical Analysis of the Energy Surface and Product Distribution

Josefredo R. Pliego, Jr. and José M. Riveros*^[a]

Abstract: The potential energy surface for the prototype solvent-free ester hydrolysis reaction: $\text{OH}^- + \text{HCOOCH}_3 \rightarrow$ products has been characterized by high level ab initio calculations of MP4/6-311 + G(2df,2p)//MP2/6-31 + G(d) quality. These calculations reveal that the approach of an OH^- ion leads to the formation of two distinct ion-molecule complexes: 1) the MS1 species with the hydroxide ion hydrogen bonded to the methyl group of the ester, and 2) the MS4 moiety resulting from proton abstraction of the formyl hydrogen by the

hydroxide ion and formation of a three-body complex of water, methoxide ion and carbon monoxide. The first complex reacts to generate formate anion and methanol products through the well known $\text{B}_{\text{AC}}2$ and $\text{S}_{\text{N}}2$ mechanisms. RRKM calculations predict that these pathways will occur with a relative contribution of 85% and 15% at 298.15 K, in excellent agreement with

experimentally measured values of 87% and 13%, respectively. The second complex reacts by loss of carbon monoxide to yield the water-methoxide complex through a single minimum potential surface and is the preferred pathway in the gas-phase. This water-methoxide adduct can further dissociate if the reactants have excess energy. These results provide clear evidence that the preferred pathways for ester hydrolysis in solution are dictated by solvation of the hydroxide ion.

Keywords: ab initio calculations • gas-phase reactions • hydrolysis

Introduction

The ability to recreate well known chemical reactions in the gas-phase under single collision conditions has made a dramatic contribution towards our understanding of intrinsic reactivity and the role that solvents play in determining chemical properties in condensed phases. This is particularly true for reactions involving ionic species for which gas-phase ion chemistry can provide valuable information regarding thermodynamic parameters, rate constants, and mechanistic details.

One of the most ubiquitous reactions that has been extensively explored in the gas-phase involves negatively charged nucleophiles with alkyl formates^[1] as prototypes of nucleophilic attack in carbonyl systems. Surprisingly enough, the most important reaction pathway for simple nucleophiles such as HO^- , RO^- , F^- , and others, corresponds to a base induced elimination of CO, with the subsequent formation of a gas-phase solvated anion as in reaction (1):

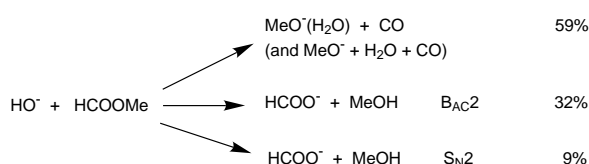


This preferred mode of reaction is particularly interesting in the case of OH^- vis-à-vis the more common process of base-catalyzed ester hydrolysis.

Ester hydrolysis plays a central role in a large number of chemical and biochemical processes.^[2] It is well known that most esters undergo basic hydrolysis by nucleophilic attack of the hydroxide ion onto the carbonyl carbon to yield a tetrahedral intermediate, namely the so-called $\text{B}_{\text{AC}}2$ mechanism. In rare cases, nucleophilic attack of the hydroxide ion on the saturated alkyl carbon leads to the final products in one step through an $\text{S}_{\text{N}}2$ or $\text{B}_{\text{AL}}2$ mechanism. While the equivalent reaction to ester hydrolysis has been well characterized in the gas-phase,^[3] two important points have emerged from such studies: a) For alkyl formates, reaction (1) and/or base induced elimination reaction promoted at the β -carbon of the alkyl group (for $\text{R} = \text{Et}$ or larger group) are preferred over conventional hydrolysis,^[1c] and b) the $\text{S}_{\text{N}}2$ pathway is competitive with the $\text{B}_{\text{AC}}2$ mechanism and can in fact be more important as shown in the CF_3COOR esters.^[3]

Results obtained in different laboratories for the gas-phase reaction of OH^- (including studies of $^{18}\text{OH}^-$) with HCOOCH_3 illustrate convincingly the qualitative and quantitative differences with solution and are summarized in Scheme 1. The disparity between the product distribution in the gas-phase and in solution clearly points out the importance of solvation effects in determining overall reactivity.

[a] Dr. J. R. Pliego, Jr., Prof. Dr. J. M. Riveros
Instituto de Química
University of São Paulo
Caixa Postal 26077, São Paulo, CEP 05513-970 (Brazil)
Fax: (+55) 11-3818-3888
E-mail: josef@iq.usp.br
jmrnigra@iq.usp.br



Scheme 1. Different gas-phase reaction mechanisms for the reaction of OH^- with HCOOCH_3 .

Large differences are also observed between the rate constants for the gas-phase and solution reactions. The most recent measurements for the gas-phase $\text{OH}^-/\text{HCOOMe}$ reaction at 298 K yield an overall rate constant of $4.4 \times 10^{10} \text{ M}^{-1} \text{ s}^{-1}$, a value close to 80% of that predicted by collision theory.^[1j] By comparison, the rate constant for the basic hydrolysis of methyl formate in aqueous solution amounts to $3.84 \times 10^1 \text{ M}^{-1} \text{ s}^{-1}$.^[4]

How can the differences illustrated above be reconciled within the realm of modern chemical thinking? On the one hand, bridging the gap between gas-phase and solution behavior from an experimental point of view remains a formidable challenge. On the other hand, the increasing reliability of present day theoretical calculations on isolated molecules and simulations of their behavior in condensed phases provide a powerful and alternative approach towards deciphering the changes observed between gas-phase and solution reactivity. For example, the effect of microsolvation on competitive gas-phase $\text{E}2$ and $\text{S}_{\text{N}}2$ reactions has been theoretically studied with density functional methods,^[5] while one of us has recently used a combination of theoretical methods to elucidate the mechanisms of some common organic reactions.^[6] Thus, studies directed towards characterizing the energy surface and dynamic features of reactions such as those shown in Scheme 1, and their solution counterpart, are very timely in our ultimate goal to properly understand solvent effects in chemical reactions. This interest is well illustrated by recent theoretical studies concerning the addition of hydroxide ion to formaldehyde,^[7] formamide,^[8] and phosphate esters^[9] in aqueous solution.

In spite of the importance of ester hydrolysis, reports aimed at describing the energy surface for these reactions are relatively few and recent. Jorgensen et al.^[10] performed the first *ab initio* theoretical calculations of the reactions shown in Scheme 1 at the $\text{HF}/4\text{-}31 + \text{G}$ level. Their results hinted that the gas-phase decarbonylation reaction is likely to proceed by a single minimum potential without an intermediate transition state and would thus be expected to be very favorable from an energetic point of view. A few years later, Pranata^[11] explored the energy surface for the $\text{S}_{\text{N}}2$ and $\text{B}_{\text{AC}2}$ mechanistic possibilities at the $\text{MP}2/6\text{-}31 + \text{G}(\text{d})/\text{HF}/6\text{-}31 + \text{G}(\text{d})$ level of theory and concluded that the $\text{B}_{\text{AC}2}$ is expected to be the more favorable pathway among these two mechanisms. Very recently, Zhan et al.^[12] have reported the gas phase potential energy surface for the reaction of the hydroxide ion with a series of esters, including methyl formate, at the $\text{MP}2/6\text{-}31 + \text{G}(\text{d},\text{p})/\text{B}3\text{LYP}/6\text{-}31 + \text{G}(\text{d},\text{p})$ level. Again, this study was primarily concerned with the reaction at the carbonyl center and explicitly addressed the question of proton exchange between the oxygen atoms of the tetrahedral intermediate.

These calculations revealed that this proton exchange has a much higher barrier than the elimination of methanol, a fact that may explain why this exchange was not observed in the gas-phase reaction.^[13]

The present report was motivated by the need to explore the energy surface for all the reaction pathways of Scheme 1 at a high level of theory coupled with statistical rate theories that could estimate the expected branching ratio for the hydrolysis reaction as a function of the internal energy of the reaction. In a second phase, we hope to report similar results for the reaction in aqueous solution in order to understand the preference for carbonyl attack in condensed phases. Calculations for the energy surface of ester hydrolysis in aqueous solutions have already attracted some attention as illustrated by two very recent calculations.^[14, 15]

Results and Discussion

Ab initio calculations: The potential energy surface for the interaction of hydroxide ions with methyl formate was investigated at the $\text{MP}2/6\text{-}31 + \text{G}(\text{d})$ level of theory. The minima and transition state structures were obtained by full geometry optimization. Harmonic frequency analysis was used to characterize the nature of the stationary points. Single point higher level energy calculations were then carried out using the $\text{MP}2/6\text{-}311 + \text{G}(2\text{df},2\text{p})$ and $\text{MP}4/6\text{-}31 + \text{G}(\text{d})$ methods. An additivity approximation of the correlation energy was used in order to obtain effective $\text{MP}4/6\text{-}311 + \text{G}(2\text{df},2\text{p})$ reaction and activation energies. The results are presented in Tables 1 and 2 and in Figures 1 to 4 and are discussed in the following section. All calculations were performed with the GAUSSIAN94 suite of programs.^[16]

Results of the ab initio calculations: Figure 1 shows the reaction steps for the interaction of hydroxide ion with methyl formate in the gas phase. Each step is numbered and the corresponding transition state for each step is identified as $\text{TS}n$.

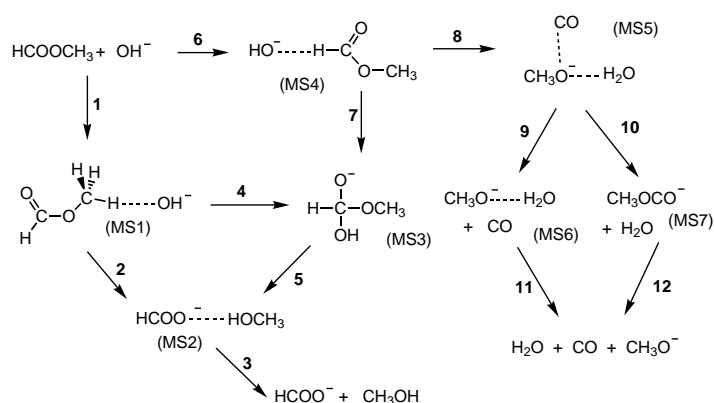


Figure 1. Pathways for the gas-phase hydrolysis reaction of OH^- with HCOOCH_3 .

The calculated structures for the minima on the energy surface relevant to the different steps and transition states are

shown in Figures 2 and 3 where only the most relevant geometric parameters are displayed for illustration purposes. Table 1 displays the calculated reaction energies at several levels of theory for the different reaction steps. Table 2 displays the calculated activation energies at different levels of theory for the different steps outlined in Figure 1. We have

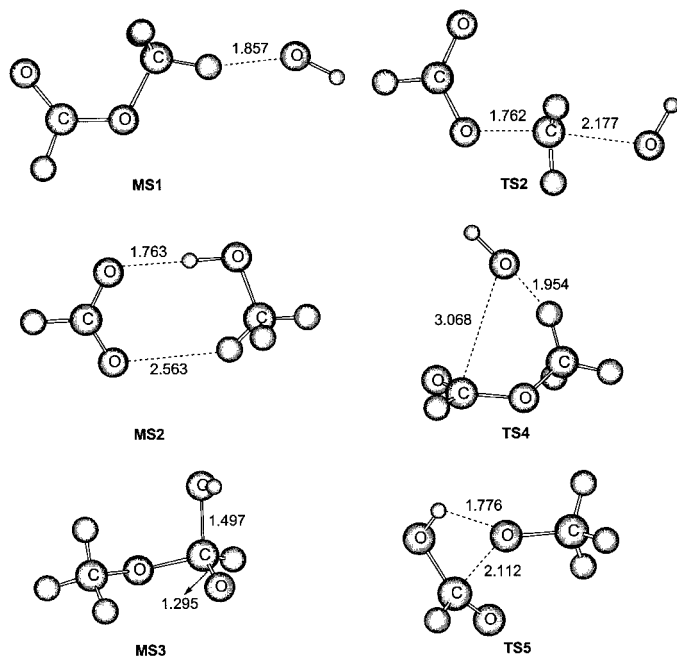


Figure 2. Structure of intermediates and transition states resulting from attachment of the hydroxide ion on the methyl group of the ester.

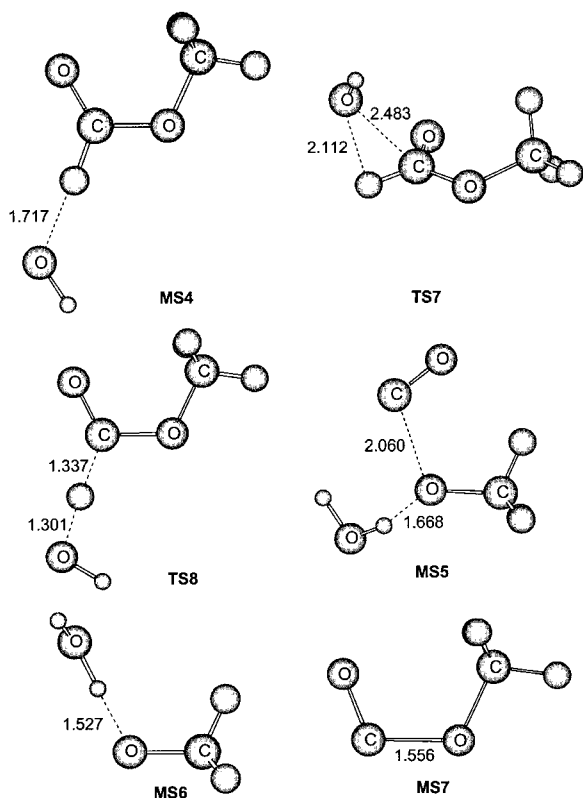


Figure 3. Structure of intermediates and transition states resulting from abstraction of the formyl hydrogen by the hydroxide ion.

only considered the most stable isomer of methyl formate, namely the Z structure^[17] which is about 6 kcal mol⁻¹ more stable than the E structure.

At the MP2/6-31 + G(d) level of theory, the interaction of an hydroxide ion with methyl formate leads to the formation of two ion–neutral complexes, MS1 and MS4. The fate of these two complexes on the energy surface can be analyzed separately:

a) The MS1 complex is predicted to be 16.5 kcal mol⁻¹ (including zero point vibrational energies) more stable than the reactants at our best level of theory (MP4/6-311 + G(2df,2p)). This complex MS1 can then proceed through steps 2 and 4.

Step 2 represents the attack of the hydroxide ion on the methyl group (the S_N2 mechanism) leading to the formate anion–methanol complex (MS2) through the TS2 local transition state. At our best level of theory, step 2 is calculated to have an activation barrier of 6.9 kcal mol⁻¹, somewhat lower than those previously calculated^[11, 12] at lower levels of electron correlation. Finally, complex MS2 can dissociate to free formate anion plus methanol and our results predict a dissociation energy of 17.7 kcal mol⁻¹.

The second reaction path available for the MS1 complex is through transition state TS4 leading to the formation of the tetrahedral intermediate (MS3). The activation barrier is small, 3.3 kcal mol⁻¹, and the tetrahedral intermediate is calculated to be very stable, 30.3 kcal mol⁻¹ below the energy of the OH⁻+HCOOCH₃ reactants. This value refers to the most stable isomer of the MS3 intermediate.^[18] Finally, step 5 represents the unimolecular elimination of methanol from the tetrahedral intermediate leading to the formate–methanol complex (MS2). This step involves a barrier amounting to 4.8 kcal mol⁻¹.

The overall exothermicity for the hydrolysis reaction is then calculated to be -42.1 kcal mol⁻¹ at 0 K which is in very good agreement with the experimental value^[19] of -39.5 ± 2.3 kcal mol⁻¹.

b) The MS4 complex (see Figure 3) is predicted to exist at the MP2/6-31 + G(d) level of theory and results from the association of the hydroxide ion to the formyl hydrogen. The classical barrier for proton abstraction from the formyl group leading to the MS5 complex amounts to 2.4 kcal mol⁻¹. However, increasing the size of the basis set and extending the level of electron correlation decreases this barrier to -0.1 kcal mol⁻¹. Inclusion of the zero point vibrational energies further decreases the barrier to -3.0 kcal mol⁻¹. Thus, these results suggest that the MS4 complex is probably not a minimum energy structure on the potential energy surface, and the approach of the hydroxide ion to the formyl hydrogen of the methyl formate is best described as leading directly to the MS5 complex. While our best level of theory is a composite energy, it is known that this additivity scheme is accurate and finds widespread use in the G1, G2, G2(MP2), and other similar methods. Furthermore, it is clear from the results in Table 2 that increasing the electron correlation from MP2 to MP4 has a very small effect on the barrier. Thus, we believe that our highest level calculations are accurate and reliable. Our conclusion is similar to that

Table 1. Reaction energies for the $\text{HCOOCH}_3 + \text{OH}^-$ process.^[a]

Step	1	2	3	4	5	6	7	8	9	10	11	12
MP2/6-31 + G*	-16.70	-45.63	19.37	-15.62	-30.01	-18.10	-14.22	-6.00	8.68	20.84	26.28	14.13
MP2/6-311 + G(2df,2p)	-17.07	-44.74	19.21	-16.01	-28.73	-18.89	-14.20	-6.46	7.74	19.44	25.86	14.16
MP4/6-31 + G*	-16.88	-45.51	19.37	-15.57	-29.94	-18.52	-13.93	-8.92	10.08	21.69	25.63	14.02
MP4/6-311 + G(2df,2p) ^[a,b]	-17.25	-44.62	19.21	-15.97	-28.65	-19.32	-13.90	-9.38	9.13	20.30	25.21	14.05
ΔZPE	0.75	1.36	-1.53	2.20	-0.84	0.38	2.57	-1.51	-2.45	-1.22	-2.05	-3.28
$\Delta E^{\text{[c]}}$	-16.50	-43.26	17.68	-13.77	-29.49	-18.94	-11.33	-10.88	6.68	19.07	23.17	10.78

[a] Energies in kcal mol^{-1} . [b] Additivity approximation. [c] Reaction energies including ΔZPE .

Table 2. Activation energies for the reaction pathways of the gas-phase $\text{HCOOCH}_3 + \text{OH}^-$ system.^[a]

Step	2	4	5	7	8
MP2/6-31 + G*	8.96	3.32	7.93	5.68	2.44
MP2/6-311 + G(2df,2p)	9.35	3.46	7.67	5.78	-0.05
MP4/6-31 + G*	7.17	2.87	7.01	5.25	2.40
MP4/6-311 + G(2df,2p) ^[b]	7.56	3.01	6.76	5.34	-0.09
ΔZPE	-0.60	0.18	-1.94	0.29	-2.95
$\Delta E^{\text{[c]}}$	6.96	3.19	4.82	5.63	-3.04

[a] Energies in kcal mol^{-1} . [b] Additivity approximation. [c] Activation energies including ΔZPE .

proposed by Jorgensen et al.^[10] based on calculations at a much lower level of theory. By comparison, Zhan et al.^[12] and Pranata^[11] have not explored this pathway. The MS5 complex is an interesting moiety since it corresponds to a methoxide ion bound to two neutral molecules, H_2O and CO. This intermediate complex can undergo dissociation through two pathways. The first possibility (steps 9 and 11) involves the loss of carbon monoxide at an expense of $6.7 \text{ kcal mol}^{-1}$ followed by fragmentation of the water-methoxide adduct (MS6) requiring an additional energy of $23.2 \text{ kcal mol}^{-1}$. This value is in excellent agreement with the reported experimental binding energy of $23.9 \text{ kcal mol}^{-1}$ for the $\text{CH}_3\text{O}^-(\text{H}_2\text{O})$ adduct.^[20] For the second pathway (steps 10 and 12), water is lost in the first step as a result of the abstraction of the formyl proton with an energy requirement of $19.1 \text{ kcal mol}^{-1}$. The anionic $^- \text{COOCH}_3$ species formed in this reaction is characterized by an oxygen(methoxide)-carbon(CO) distance of 1.556 \AA that is indicative of covalent bonding. By comparison, this same distance is calculated to be 2.060 \AA in the $[\text{CH}_3\text{O}^-\text{O}]$ moiety of the MS5 complex. However, the $^- \text{COOCH}_3$ carbanion can further decompose to carbon monoxide and methoxide ion with an endothermicity of $10.8 \text{ kcal mol}^{-1}$ (step 12). The energy of the $\text{CO} + \text{CH}_3\text{O}^- + \text{H}_2\text{O}$ products is calculated to lie $0.03 \text{ kcal mol}^{-1}$ above that of the $\text{OH}^- + \text{HCOOCH}_3$ reactants. This value should be compared with the experimental overall endothermicity of $3.1 \pm 1.1 \text{ kcal mol}^{-1}$.^[19]

Another possible pathway involves transition state TS7 and connecting the MS4 complex to the MS3 tetrahedral intermediate. However, since the MS4 structure does not survive as a minimum at higher level of theory, TS7 must connect the MS5 complex to the MS3 intermediate. The energy barrier for this latter pathway is calculated to be $16.5 \text{ kcal mol}^{-1}$.

Qualitative analysis of the gas phase reaction pathways: While a rigorous analysis of the $\text{OH}^-/\text{HCOOMe}$ reaction would ideally be based on dynamic calculations similar to those used for gas-phase $\text{S}_{\text{N}}2$ reactions,^[21] this is still a very complex task for a system with so many reaction channels. An alternative approach is to apply statistical unimolecular rate theory to the intermediates of these ion/molecule reactions. Since gas phase ion-molecule reactions are typically studied at low pressures using techniques such as ion cyclotron resonance or flowing afterglow, the fate of intermediate ion-molecule complexes can be treated within the realm of a microcanonical ensemble. In this section we initially make a qualitative analysis of the reaction system to predict which products should be observed based on the ab initio calculations. In the next section, we present an RRKM calculation of the rate constant for rearrangement of the MS1 complex to predict the branching ratio between the $\text{S}_{\text{N}}2$ mechanism and the $\text{B}_{\text{AC}}2$ mechanism for the gas-phase reaction.

Figure 4 summarizes the results for the potential energy surface profile of the $\text{OH}^- + \text{HCOOCH}_3$ system in the gas-phase. A static approach along this energy surface reveals that the approximation of the hydroxide ion to the methyl formate leads to a decrease of the potential energy and initial formation of the MS1 and MS4 (and MS5) complexes as the most probable events. In fact, when we freeze the oxygen-(hydroxide)-oxygen(ester) distance at 5 \AA and subsequently optimize the remaining geometrical variables, the system relaxes to structures similar to the MS1 and MS4 complexes. The direct approach of the hydroxide ion to the carbonyl carbon leading to tetrahedral intermediate (MS3) also proceeds without a formal energy barrier. However, direct formation of MS3 is expected to have a low probability since it requires a very specific orientation of the colliding species in the collision event. These considerations suggest that gas-phase collisions between a hydroxide ion and the ester will lead preferentially to either complex MS1 or MS5 with only a small fraction of collisions probably leading directly to the tetrahedral intermediate (MS3). Thus, the product distribution can be viewed as being dictated by the unimolecular fragmentation of the long lived MS1 and MS5 complexes.

Complex MS1 is formed with at least $16.50 \text{ kcal mol}^{-1}$ of internal energy. Thus, this complex is expected to proceed readily along pathways 2 and 4 which are characterized by energy barriers of 6.9 and $3.2 \text{ kcal mol}^{-1}$, respectively. For systems that can be adequately described by statistical rate theories, the branching ratio for these two channels will depend on the number of states of the respective transition states. Reaction through TS2 leads to the MS2 complex which

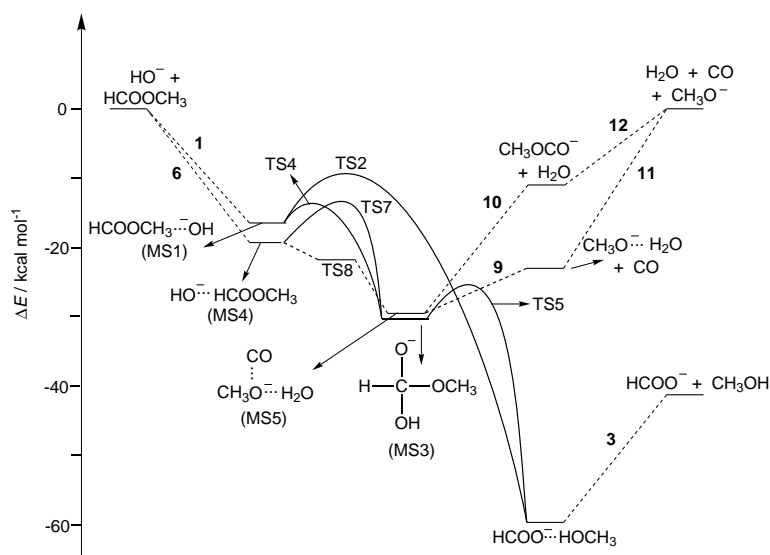


Figure 4. Calculated energy profile of the gas-phase $\text{OH}^- + \text{HCOOCH}_3$ reaction.

is located $59.8 \text{ kcal mol}^{-1}$ below the energy of the reagents. In the absence of thermalizing collisions, these energy-rich MS2 ion-neutral complexes are expected to undergo facile dissociation to methanol and formate anion, predicted to be $17.7 \text{ kcal mol}^{-1}$ above MS2. The other pathway, namely reaction through step 4, leads to the tetrahedral intermediate (MS3) which is located $30.3 \text{ kcal mol}^{-1}$ below the energy of the reactants. This species can then proceed to the MS2 complex through TS5, and a barrier of $4.8 \text{ kcal mol}^{-1}$, and finally dissociate to methanol plus formate anion. Thus, both the $\text{S}_{\text{N}}2$ and $\text{B}_{\text{AC}}2$ mechanism arise from a common intermediate, MS1, to yield the products of gas-phase hydrolysis.

The (MS5) complex, located $29.8 \text{ kcal mol}^{-1}$ below the energy of the reactants, has two possible dissociation pathways. Step 9 involves the loss of CO and formation of the solvated anion $\text{CH}_3\text{O}^-(\text{H}_2\text{O})$ and requires only $6.7 \text{ kcal mol}^{-1}$, while the loss of H_2O through step 10 requires $19.1 \text{ kcal mol}^{-1}$. The large difference in energy requirements for these two channels suggests that observation of proton abstraction to yield $^-\text{CO}_2\text{CH}_3$ (MS7) is unlikely in this case although the actual branching ratio will also depend on the number of states for each generalized transition state. The fact that proton abstraction is not observed experimentally^[1] is in agreement with our prediction that formation of the MS6 complex plus carbon monoxide are the major products. It is also reasonable to expect that further dissociation of the MS6 complex to yield $\text{CH}_3\text{O}^- + \text{H}_2\text{O}$ as final products would be a very sensitive function of the energy content of the reactants. These predictions are fully borne out by the experimental observations.^[1c] In addition to these dissociation channels, rearrangement through TS7 is another possibility. However, due to the high barrier of $16.5 \text{ kcal mol}^{-1}$ for this step compared with $6.7 \text{ kcal mol}^{-1}$ for step 9 and the tighter characteristics of the transition state TS7, this pathway should not play an important role in the fate of the MS5 complex.

RRKM calculations for the $\text{B}_{\text{AC}}2$ and $\text{S}_{\text{N}}2$ rate constants: The use of RRKM calculations on intermediate complexes to determine the efficiency of ion/molecule reactions proceeding

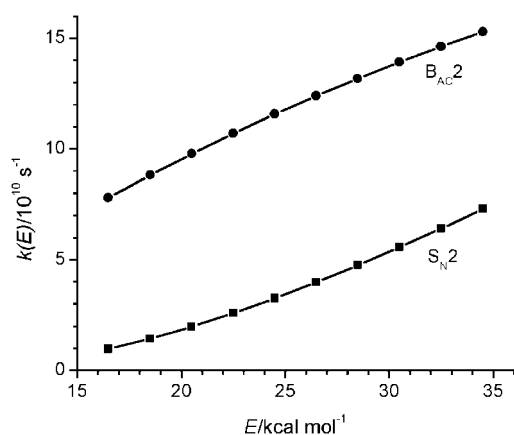
through double well potential energy surfaces was first applied by Brauman and co-workers in their classical study of gas-phase $\text{S}_{\text{N}}2$ reactions,^[22] and later extended to gas-phase nucleophilic reactions in carbonyl systems.^[23] This approach has been successful in providing a quantitative interpretation of the outcome of these reactions. Nevertheless, recent dynamic calculations on gas-phase $\text{S}_{\text{N}}2$ reactions reveal that results obtained from this type of straightforward statistical rate theory approach must be viewed with caution because of the possibility of poor coupling between the low-frequency vibrations associated with complex formation and the rest of system, and insufficient time for proper internal energy redistribution.^[24] In the present case, an estimate of the overall efficiency of the reaction is more difficult because it would be necessary to have some dynamical information on the trajectories and their partition between the MS1 and MS5 complexes. This in turn is necessary to make an estimate of the branching ratio of all reaction channels. On the other hand, considerable insight can be gained by looking at the fate of each complex.

Since formation of $\text{CH}_3\text{O}^-(\text{H}_2\text{O})$ and CO (or the dissociated products) proceeds along a single minimum surface according to our highest level calculation, an estimate of the efficiency of MS5 to proceed through step 9 as opposed to returning to reactants could be modeled by RRKM calculations by using variational transition state theory for both cases. Yet, this calculation does not provide much insight on the overall product distribution and was not pursued in the present study.

On the other hand, the branching ratio for the $\text{S}_{\text{N}}2$ and the $\text{B}_{\text{AC}}2$ mechanisms can be estimated by adequate modeling of the unimolecular decomposition of MS1 along steps 2 and 4 and calculation of the corresponding rate constants. This is an important consideration for comparing gas-phase with solution behavior. Thus, we have used RRKM theory^[25] to calculate the unimolecular rate constants for steps 2 and 4 assuming that the system can be described by a statistical theory. The necessary energy and vibrational data to perform these calculations were generated by our ab initio calculations and the relevant parameters are shown in Table 3. The Zhu and Hase program^[26] was used for the RRKM calculations by considering $J=0$. The results are presented in Figures 5 and 6, where the unimolecular rate constants and the relative yield for steps 2 and 4 are calculated as a function of the internal energy of the MS1 complex. A degeneracy of two was used for the reaction path corresponding to step 4 due to the possibility of the hydroxide ion approaching the carbonyl center either from above or below. For both cases, the rate constants increase with energy but the relative yield reveals

Table 3. Harmonic vibrational frequencies (in cm^{-1}) obtained at the MP2/6-31 + G(d) level of theory and used in the RRKM calculations.

MS1	TS2	TS4
39	88	110
66	125	195
69	155	232
191	184	244
238	305	272
275	352	289
329	357	358
351	591	764
777	775	938
888	1047	1024
1042	1114	1207
1210	1150	1231
1225	1218	1278
1291	1339	1431
1434	1427	1480
1528	1435	1522
1556	1443	1579
1568	1704	1761
1753	2967	3001
2972	3234	3126
3090	3431	3157
3172	3433	3209
3216	3717	3730
3732		

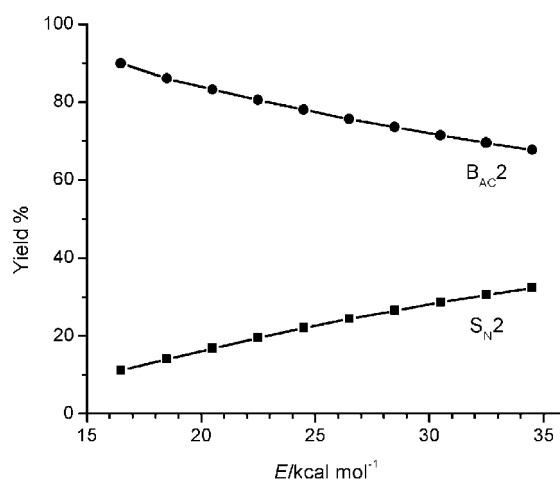
Figure 5. Calculated unimolecular rate constants for the MS1 complex to undergo the $B_{AC}2$ and S_N2 reactions as a function of internal energy.

that the $B_{AC}2$ mechanism decreases at higher internal energy. At the lowest energy possible of $16.50 \text{ kcal mol}^{-1}$ the yields of the S_N2 and $B_{AC}2$ mechanism are 11.1% and 88.9%, while at $30.5 \text{ kcal mol}^{-1}$ the yields become 28.6% and 71.4%, respectively.

In order to compare our theoretical calculations with the experimental data, it is necessary to determine the amount of energy available to the MS1 complex. At thermal equilibrium at 298.15 K, the MS1 complex will have an energy E^* :

$$E^* = \Delta E_{MS1} + \Delta E_R - \Delta E_{MS1}$$

where E^* is the energy available for reaction, ΔE_{MS1} is the energy released upon formation of MS1 including zero point vibrational energy, E_R is the thermal contribution to the energy of the reactants, and E_{MS1} is the thermal rotational and translational energy of the MS1 complex. These values amount to $\Delta E_{MS1} = 16.50 \text{ kcal mol}^{-1}$, $E_R = 4.30 \text{ kcal mol}^{-1}$,

Figure 6. Calculated relative yield of the $B_{AC}2$ and S_N2 mechanism for the gas-phase reaction $\text{OH}^- + \text{HCOOCH}_3 \rightarrow \text{HCOO}^- + \text{CH}_3\text{OH}$.

$E_{MS1} = 1.78 \text{ kcal mol}^{-1}$, resulting in $E^* = 19.0 \text{ kcal mol}^{-1}$. Using this energy value, we find that the yields of the S_N2 and $B_{AC}2$ mechanisms are 15% and 85%, respectively. This calculation is in excellent agreement with the value obtained by DePuy et al.^[1f, 1g] of 13% and 87%, but lower than the 27% and 73% values obtained in these laboratories.^[3] Since the measurements in our laboratory were based on drift cell ion cyclotron resonance experiments, it is quite likely that the ions in our experiments were not fully thermalized. The higher contribution of the S_N2 reaction in our case is in fact consistent with the expected behavior for the intermediate complex MS1 at higher levels of internal energy.

Conclusion

The results obtained in the present calculations provide a high level description of the energy surface relevant to the gas-phase hydrolysis reaction. Furthermore, the combination of these calculations with simple RRKM calculations on the reaction intermediates provides excellent agreement with the observed experimental product distribution between the S_N2 and $B_{AC}2$ mechanisms. These results also point out that proper interpretation of these mechanistic details requires not only the characterization of the overall energy surface of the reaction but some consideration of the actual dynamics of the processes.

How can these results be interpreted qualitatively to the behavior in condensed phases? Hydroxide ions are known to form a very stable complex with one water molecule, and studies of hydroxide ion–water clusters show that the hydroxide ion can support up to four water molecules inside its first coordination shell.^[27, 28] Thus, in a strongly solvating medium such as H_2O , the water molecules deactivate the highly reactive hydroxide ion. As a consequence, many reactions involving the hydroxide ion in aqueous solution are slow and its basicity is considerably decreased. Thus, abstraction of the formyl hydrogen is expected to be much less favorable and in fact becomes unimportant in condensed phases. These differences and a more elaborate explanation of

the effect of solvation on the two channels for ester hydrolysis will be the subject of an upcoming report.

Acknowledgement

The authors wish to thank the support of the São Paulo Science Foundation (FAPESP), the Brazilian Research Council (CNPq), and the Laboratory for Advanced Computation (LCCA) of the University of São Paulo.

- [1] a) L. K. Blair, P. C. Isolani, J. M. Riveros, *J. Am. Chem. Soc.* **1973**, *95*, 1057; b) P. C. Isolani, J. M. Riveros, *Chem. Phys. Lett.* **1975**, *33*, 362; c) J. F. G. Faigle, P. C. Isolani, J. M. Riveros, *J. Am. Chem. Soc.* **1976**, *98*, 2049; d) M. Comisarow, *Can. J. Chem.* **1977**, *55*, 171; e) J. E. Bartmess, R. L. Hays, G. Caldwell, *J. Am. Chem. Soc.* **1981**, *103*, 1338; f) C. H. DePuy, E. W. Della, J. Filley, J. J. Grabowski, V. M. Bierbaum, *J. Am. Chem. Soc.* **1983**, *105*, 2480; g) C. L. Johlman, C. L. Wilkins, *J. Am. Chem. Soc.* **1985**, *107*, 327; h) C. H. DePuy, J. J. Grabowski, V. V. M. Bierbaum, S. Ingemann, N. M. M. Nibbering, *J. Am. Chem. Soc.* **1985**, *107*, 1093; i) H. van der Wel, N. M. M. Nibbering, *Recl. Trav. Chim. Pays-Bas* **1988**, *107*, 479; j) B. T. Fink, C. M. Hadad, *J. Chem. Soc. Perkin Trans. 2* **1999**, 2397.
- [2] For some classical reviews, see a) M. L. Bender, *Chem. Rev.* **1960**, *60*, 53; b) W. P. Jencks, *Prog. Phys. Org. Chem.* **1964**, *2*, 63; c) E. H. Cordes, H. G. Bull, *Chem. Rev.* **1974**, *74*, 581; d) W. P. Jencks, *Acc. Chem. Res.* **1980**, *13*, 161.
- [3] K. Takashima, J. M. Riveros, *J. Am. Chem. Soc.* **1978**, *100*, 6128.
- [4] H. M. Humphreys, L. P. Hammett, *J. Am. Chem. Soc.* **1956**, *78*, 521.
- [5] F. M. Bickelhaupt, E. J. Baerends, N. M. M. Nibbering, *Chem. Eur. J.* **1996**, *2*, 196.
- [6] a) J. R. Pliego Jr., W. B. de Almeida, *J. Phys. Chem. A* **1999**, *103*, 3904; b) J. R. Pliego Jr., W. B. de Almeida, *Phys. Chem. Chem. Phys.* **1999**, *1*, 1031; c) J. R. Pliego Jr., M. A. França, W. B. de Almeida, *Chem. Phys. Lett.* **1998**, *285*, 121.
- [7] J. D. Madura, W. L. Jorgensen, *J. Am. Chem. Soc.* **1986**, *108*, 2517.
- [8] D. Bakowies, P. A. Kollman, *J. Am. Chem. Soc.* **1999**, *121*, 5712.
- [9] A. Dejaegere, X. Liang, M. Karplus, *J. Chem. Soc. Faraday Trans.* **1994**, *90*, 1763.
- [10] W. L. Jorgensen, J. F. Blake, J. D. Madura, S. G. Wierschke, *ACS Symp. Ser.* **1987**, *353*, 200.
- [11] J. Pranata, *J. Phys. Chem.* **1994**, *98*, 1180.
- [12] C.-G. Zhan, D. W. Landry, R. L. Ornstein, *J. Am. Chem. Soc.* **2000**, *122*, 1522.
- [13] K. Takashima, S. M. Jose, A. T. do Amaral, J. M. Riveros, *J. Chem. Soc. Chem. Commun.* **1983**, 1255.
- [14] F. Haeflner, C.-H. Hu, T. Brinck, T. Norin, *THEOCHEM* **1999**, *459*, 85.
- [15] C.-G. Zhan, D. W. Landry, R. L. Ornstein, *J. Am. Chem. Soc.* **2000**, *122*, 2621.
- [16] *Gaussian 94*, Revision D.2, Gaussian, Inc., Pittsburgh, PA, **1995**.
- [17] K. B. Wiberg, K. E. Laidig, *J. Am. Chem. Soc.* **1987**, *109*, 5935.
- [18] C. S. Ewig, J. R. Van Wazer, *J. Am. Chem. Soc.* **1986**, *108*, 4774.
- [19] The exothermicity was calculated from the experimental heats of formation tabulated in the NIST Standard Reference Database Number 69 - February 2000 Release. See <http://webbook.nist.gov/chemistry/>
- [20] M. Meot-Ner(Mautner), *J. Am. Chem. Soc.* **1986**, *108*, 6189.
- [21] W. L. Hase, *Science* **1994**, *266*, 998.
- [22] W. N. Olmstead, J. I. Brauman, *J. Am. Chem. Soc.* **1977**, *99*, 4219.
- [23] O. I. Asubiojo, J. I. Brauman, *J. Am. Chem. Soc.* **1979**, *101*, 3715.
- [24] T. Baer, W. L. Hase, *Unimolecular Reaction Dynamics. Theory and Experiments*, Oxford University Press, New York, NY, **1996**.
- [25] For some recent examples and discussion of this problem, see a) H. Wang, W. L. Hase, *J. Am. Chem. Soc.* **1997**, *119*, 3093; b) H. Wang, G. H. Peslherbe, W. L. Hase, *J. Am. Chem. Soc.* **1994**, *116*, 9644; c) S. T. Graul, M. T. Bowers, H. Wang, W. L. Hase, *J. Am. Chem. Soc.* **1994**, *116*, 3875.
- [26] L. Zhu, W. L. Hase, *A General RRKM Program* Department of Chemistry, Wayne State University, **1993**.
- [27] J. R. Pliego Jr., J. M. Riveros, *J. Chem. Phys.* **2000**, *112*, 4045.
- [28] S. X. Xantheas, *J. Am. Chem. Soc.* **1995**, *117*, 10373.

Received: June 13, 2000 [F2540]